

# NEDLA TEST SITE REPORT

## Chita Site

Tatiana Loboda <sup>1</sup>, Ivan Csiszar <sup>2</sup>

<sup>1</sup> University of Maryland, Geography Department

<sup>2</sup> NOAA/NESDIS Center for Satellite Applications and Research

### Contents

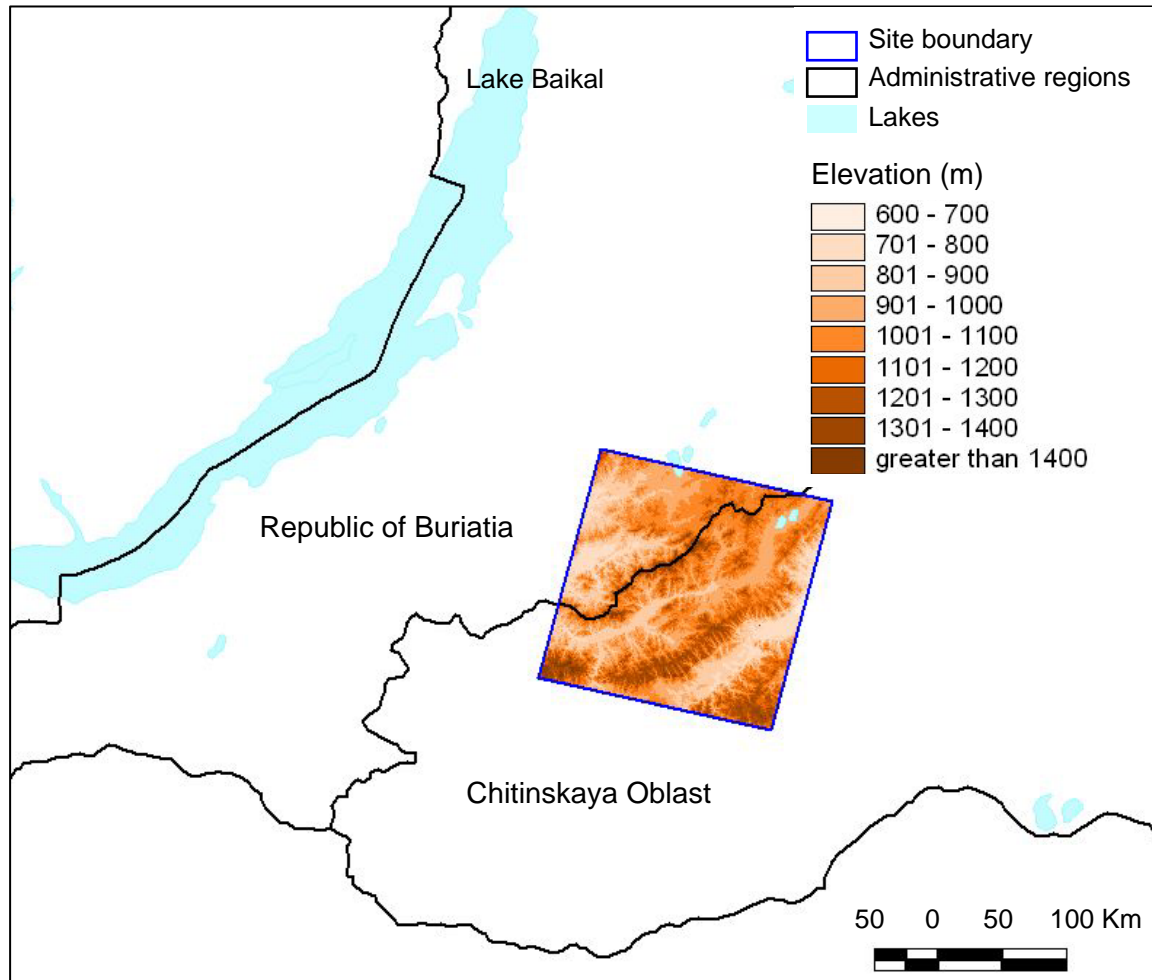
<b>1</b>	<b>Site Location</b>	<b>3</b>
1.1	Country, State, Province	3
1.2	Center coordinates	3
1.3	Geographic settings and environmental characteristics	3
1.4	Land Use	4
1.5	Major types of vegetation disturbance and land cover change	5
<b>2</b>	<b>Satellite Imagery</b>	<b>5</b>
2.1	Landsat imagery	5
2.2	ASTER imagery	5
<b>3</b>	<b>Auxiliary data</b>	<b>6</b>
<b>4</b>	<b>Mapping Legend</b>	<b>6</b>
<b>5</b>	<b>Land Cover Map</b>	<b>8</b>
5.1	Pre-processing	8
5.2	Land cover classification	9
5.2.1	Masks	9
5.2.2	Development of metrics for image classification	9
5.2.3	Mapping levels of post-fire tree mortality	10
5.2.4	Separation of major land cover types	10
5.2.5	Mapping vegetation classes	10
5.3	Post-classification processing	10
5.3.1	Identification of subclasses for the Bare and Herbaceous groups	10
5.3.2	Final classification post-processing	11
5.4	Accuracy assessment	11
5.4.1	Aggregated classes accuracy assessment	11
5.4.2	Full classification accuracy assessment	11
5.5	Analysis of mapping results	14
5.6	Comparison to coarse resolution land cover maps	15
<b>6</b>	<b>Land Cover Change Map</b>	<b>17</b>
6.1	Pre-processing	17
6.1.1	Mature forest mapping	18
6.1.2	Accuracy assessment for mature forest mapping	18
6.1.2.1	Scene from May 29, 1992	18
6.1.2.2	Scene from August 7, 2006	19

<b>6.2</b>	<b>Change detection</b> .....	19
<b>6.3</b>	<b>Post-classification processing</b> .....	20
<b>6.4</b>	<b>Accuracy assessment</b> .....	20
<b>6.4.1</b>	<b>Random selection accuracy assessment</b> .....	20
<b>6.4.2</b>	<b>Analyst driven selection accuracy assessment</b> .....	21
<b>6.5</b>	<b>Results of the land cover change map</b> .....	22
<b>6.6</b>	<b>Analysis of the land cover change map</b> .....	23
<b>7</b>	<b>Publications Using the Site Data</b> .....	25
<b>8</b>	<b>List of Contributors to Site Data and Report</b> .....	25
<b>9</b>	<b>Acknowledgements</b> .....	25
<b>10</b>	<b>References</b> .....	25

# 1 Site Location

## 1.1 Country, State, Province

The test site is located within the Russian Federation on the borderline between the Republic of Buriatia and Chitinskaya Oblast.



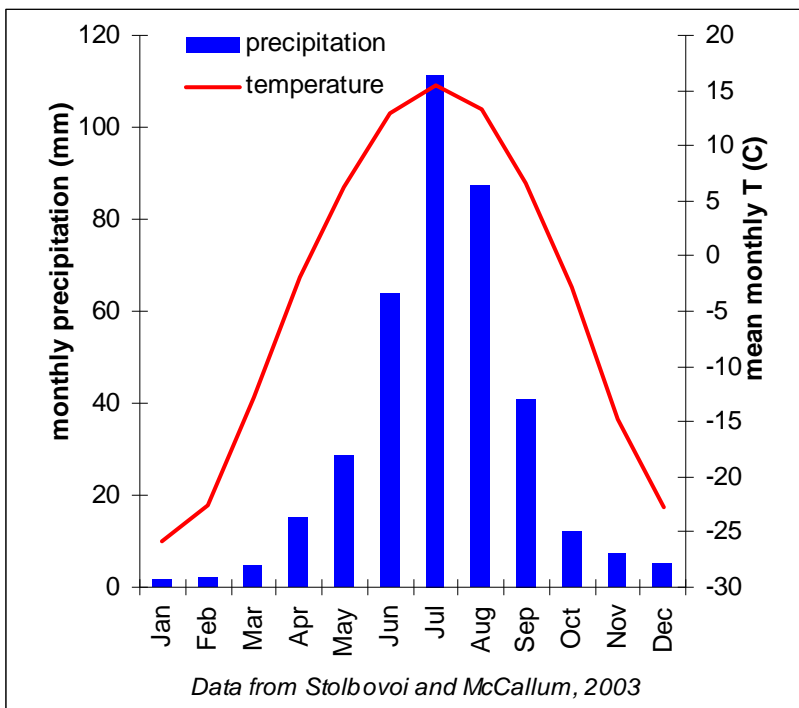
## 1.2 Center coordinates

57.7° N, 111.6° E (Landsat WRS2 path 129 row 24)

## 1.3 Geographic settings and environmental characteristics

The site is found in the southern part of Eastern Siberia to the east of Lake Baikal. The site spans across several chains of the Zabaikalye Mountain system around Yablonovy Mountain Range with the elevations ranging between 600 and 1500 m and individual peaks reaching 1681 m (Kusotuy Mountain). The region's ecosystems developed cold climatic conditions with mean annual temperature of -4 °C and mean January temperatures around -26 °C and mean July temperatures around 15 °C (Stolbovoi and McCallum, 2003). Despite the position of the site

deeply within the Siberian continent the test site receives ~380 mm of rainfall per year with the major peak during summer months. The area experiences roughly between 95 and 120 frost-free



days per year depending on the elevation of the area above sea level. The duration of vegetative period becomes shorter with the increase in the altitude. However, the exact number of frost-free days is also determined by the exposition of the slopes and relief configuration.

Mountain valleys of the study site host five major rivers including Uda, Khudan, Khilok, Olenguy, and Ingoda and multiple lakes of difference sizes. The ecosystems of this test site developed within the zone of discontinuous permafrost (50-90% permafrost extent) and ice thickness of less than 20 cm (Stolbovoi and McCallum, 2003). Despite the wide spread of permafrost within the site ~50% of the soils are well drained, 23% are moderately-well drained, 7% are moderately-poorly drained, 14% are poorly drained and 6% are excessively drained (based on soil properties data in Stolbovoi and McCallum, 2003). The poorly drained soils of the Khilok river valley frequently correspond to swamped areas with shallow (30-50cm) peat accumulation. On average soil carbon density of the top 30 cm of the soil is ~ 64 C kg/m<sup>2</sup>.

The site represents predominantly tree-dominated landscapes with larch, pine and birch among the dominate tree species. The northern part of the test site includes extensive shrub dominated communities covered with dwarf birch. River valleys are largely non-forested.

#### 1.4 Land Use

The land use within the Chita study site is represented by two major activities – agriculture (including croplands and natural forage land) and forest industry (Stolbovoi and McCallum,

2003). Major river valleys are predominantly used for crop cultivation which accounts for 20 – 50% of valley land cover and include natural meadow or steppe forage land and some forests. The majority of croplands are used for grain (wheat) production with additional subsidiary farming on smaller plots of land. The majority of the forested areas are considered “forest of limited exploitation (group II)” and only south-eastern section of the study site is covered by “exploited forest (group III)” forest class.

### 1.5 Major types of vegetation disturbance and land cover change

The major type of vegetation disturbance and land cover change is caused by wildland fire (Stolbovoi and McCallum, 2003). Fire is a natural component of boreal forest ecosystems driving forest succession necessary to ensure long-term ecosystem well-being. On average there are 101.575 fires per 1,000,000 ha per year occurred within the study site; however fire frequency is considerably higher in denser populated north-east of the area (~245 fires per 1,000,000 ha per year) compared to the rest of the area (ranging from 32 to 77 fires per 1,000,000 ha per year). These fires were reported to burn on average ~0.73 % of the forested areas annually between 1987 and 2000. In addition to fire-induced disturbance, commercial logging represents the second most prominent disturbance agent.

## 2 Satellite Imagery

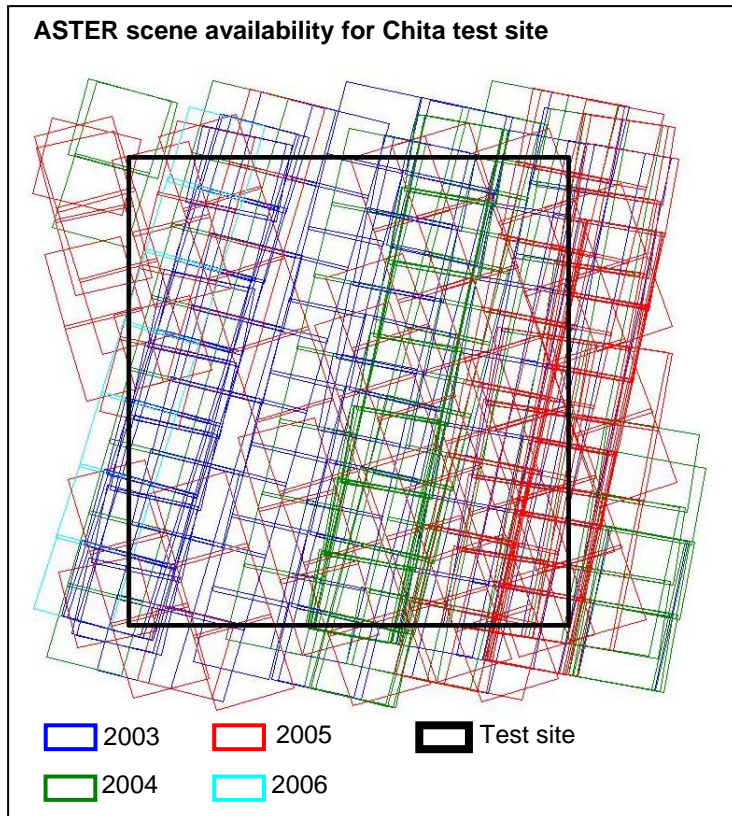
### 2.1 Landsat imagery

Landsat MSS, TM, and ETM+ images present the primary source of data for land cover mapping and change detection. The image stack includes 10 images and covers the time period between 1976 and 2006.

Instrument	Acquisition date	Use	Notes
MSS	8/22/1976	primary	change detection basis
TM	1/4/1989	secondary	winter scene auxiliary for classification
TM	7/18/1990	secondary	striping in across the lower part of the image
TM	5/28/1992	primary	change detection basis
ETM+	6/11/2000	primary	classification basis, change detection basis
ETM+	6/1/2002	secondary	post-fire vegetation regrowth
ETM+	5/19/2003	secondary	post-fire vegetation regrowth
ETM+	6/6/2004	secondary	post-fire vegetation regrowth
ETM+	6/25/2005	secondary	post-fire vegetation regrowth
TM	8/7/2006	primary	change detection basis

### 2.2 ASTER imagery

Aster images were obtained to map the extent of fire occurrence in 2003, map vegetation mortality, and post-fire vegetation regrowth.








### 3 Auxiliary data

QuickBird images available at GoogleEarth were visually examined to identify sites for urban areas and cultivated lands as well as in defining training and validation pixels for the classification. In addition, the Shuttle Radar Topography Missions (SRTM) dataset was used to identify potentially cultivated lands (slope < 5%).



### 4 Mapping Legend

The following land cover classes consistent with the NELDA Land Cover Legend were identified within the scene.

Class_ID	Description	Examples
1	Tree.needleleaf.deciduous.closed	
2	Tree.needleleaf.deciduous.open	
3	Tree.mixed.closed	

4	Tree.mixed.open	
5	Tree.broadleaf.deciduous.closed	
6	Tree.broadleaf.deciduous.open	
7	Tree.mortality.low (stands with 20% or less of fire induced mortality)	
8	Tree.mortality.moderate (stands with 20 - 60% of fire induced mortality)	
9	Tree.mortality.high (stands with greater than 60% of fire induced mortality)	

---

10	Shrub.broadleaf.closed	
11	Shrub.broadleaf.open	
12	Shrub.mortality	

---

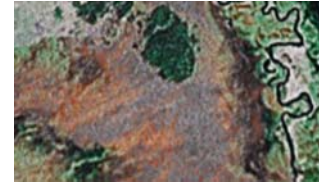
13	Herbaceous	
----	------------	---

14 Herbaceous.cultivated



---

15 Bare.sparse  
(bare and sparsely vegetated lands)



16 Bare.built  
(bare lands with presence of build up)



---

17 Water



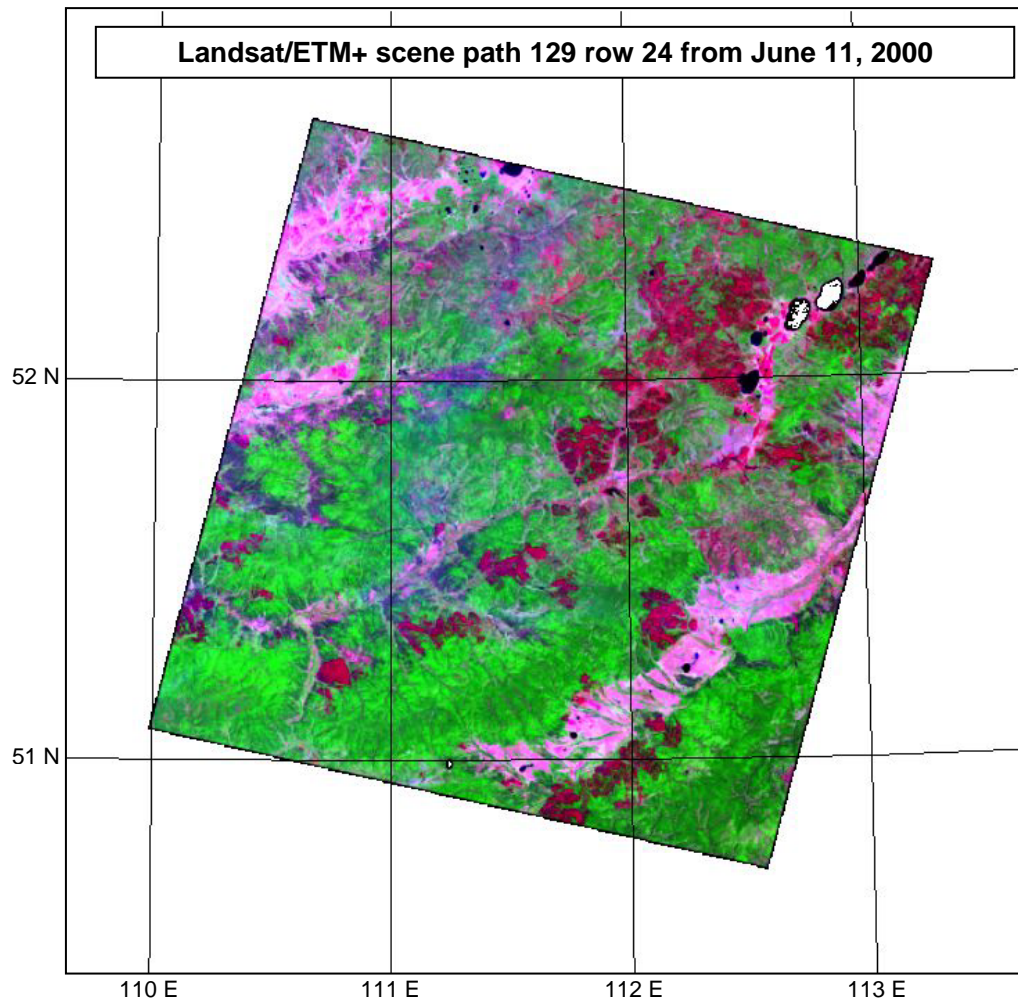
---

## 5 Land Cover Map

### 5.1 Pre-processing

Landsat TM and ETM+ imagery was preprocessed through the standard LEDAPS systems (<http://ledaps.nascom.nasa.gov/ledaps/docs1.html>). The LEDAPS system outputs orthorectified and atmospherically corrected images converted to surface reflectance values. The images involved in Land cover classification and change detection were additionally co-registered with the accuracy < 0.5 pixels.





## 5.2 Land cover classification

### 5.2.1 Masks

Several masks developed prior to classifying the image to eliminate potential confusion of classes:

- i) background mask – areas of the image which contain no valid data values
- ii) water mask – thresholded in NIR and hand digitized
- iii) fresh burns were mapped using supervised Spectral Angle Mapping approach and MODIS active fire detections (see specific description of the approach in Loboda et al., 2007)

### 5.2.2 Development of metrics for image classification

Additional metrics were calculated to support decision tree application:

- i) Normalized Burn Ratio (NBR)

- ii) NDVI
- iii) Principal Components
- iv) Tasseled Cap (using surface reflectance indices published in Crist, 1985)

These metrics and the original 7 bands (including resampled thermal band (standard output of LEDAPS) were stacked in one file.

### 5.2.3 Mapping levels of post-fire tree mortality

Post-fire tree mortality was mapped using the burn severity mapping approach adopted by the US Department of Interior (Key and Benson, 1999). The difference Normalized Burn Ratio (dNBR) was calculated by differencing NBR between pre-burn image of 1992 and the post-burn image of 2000 within the area masked as “recent burns”. The resultant dNBR values were classified into the 4 burn severity groups and, subsequently, tree mortality was estimated using the reverse interpretation of the relationship between dNBR and the Composite Burn Index (CBI) – a field based measure of burn severity (Key and Benson, 1999).

### 5.2.4 Separation of major land cover types

A decision tree was used to separate (with the best visual accuracy) water, bare land, vegetated areas ( $ndvi > 0.25$ ), and special cases (e.g. fresh burns) using masks, stacked metrics described above.

### 5.2.5 Mapping vegetation classes

- i) Training samples for visually identifiable in high resolution (Quickbird available at Google Earth) and multi-temporal images (winter image from 1/4/1989 and the classification image from 6/11/2002) were selected across the classification scene.
- ii) Training spectra for each class from the full stack of classification metrics were extracted and reformatted for further processing in the statistical software
- iii) S-Plus statistical package was used to develop a decision tree algorithm
- iv) the decision tree rules were implemented within the “vegetative cover” mask (see section 5.2.4)

## 5.3 Post-classification processing

### 5.3.1 Identification of subclasses for the Bare and Herbaceous groups

A “potentially cultivated lands” layer was developed through a combination of several techniques:

- i) slopes  $< 5\%$  were extracted from the SRTM dataset into the “potentially cultivated” layer
- ii) the “potentially cultivated” layer was further adjusted to match the approximate boundaries of cultivated lands visible in the base image and Google Earth
- iii) approximate outlines of urban areas were obtained from Google Earth maps
- iv) **bare and herbaceous lands** within “potentially cultivated” were assigned to the **Herbaceous.cultivated** class (based on the assumption that those area will be herbaceous dominated at least 1 month out of the year).
- v) **Bare and herbaceous lands** within “potentially urban” areas were assigned to **Bare.built**

- vi) **bare lands** outside the “potentially cultivated” or “urban” areas were assigned to **Bare.sparse**

### 5.3.2 Final classification post-processing

The developed classes from all steps of classification were combined into a single classification scheme according to legend presented in section 4. The resultant land cover map was sieved following the “>= 5 contiguous pixels” rule to eliminate speckle. The filtered pixels were assigned a max value from a 5X5 or 7X7 matrix.

## 5.4 Accuracy assessment

Accuracy assessment was conducted following the accuracy assessment protocol developed by Dr. Krankina. It presents a combination of in situ data and randomly distributed additional points in classes that are poorly represented by ground data. The distribution of the accuracy assessment points overall proportional to the areal distribution of the mapped classes and consists of minimum of 300 randomly selected points across the image. For classes, where the proportional representation of 300 total points results in a sample of fewer than 30 points, additional random points are added to a minimum of 30 points in a sample class. According to the protocol two types of accuracy assessment are presented: 1) an assessment for 5 aggregated land cover classes including trees, shrubs, herbaceous cover, barren lands, and water; and 2) an assessment for the full set of classes identified within the site.

### 5.4.1 Aggregated classes accuracy assessment

For the accuracy assessment of the aggregated classes random points across the full extent of the classification were selected proportionally to the area of the class but no less than 30 pixels per class (see section 5.4). These random points were further assigned by the analyst to one of the 5 aggregated classes based on the surface reflectance characteristics and high resolution QuickBird images available at Google Earth.

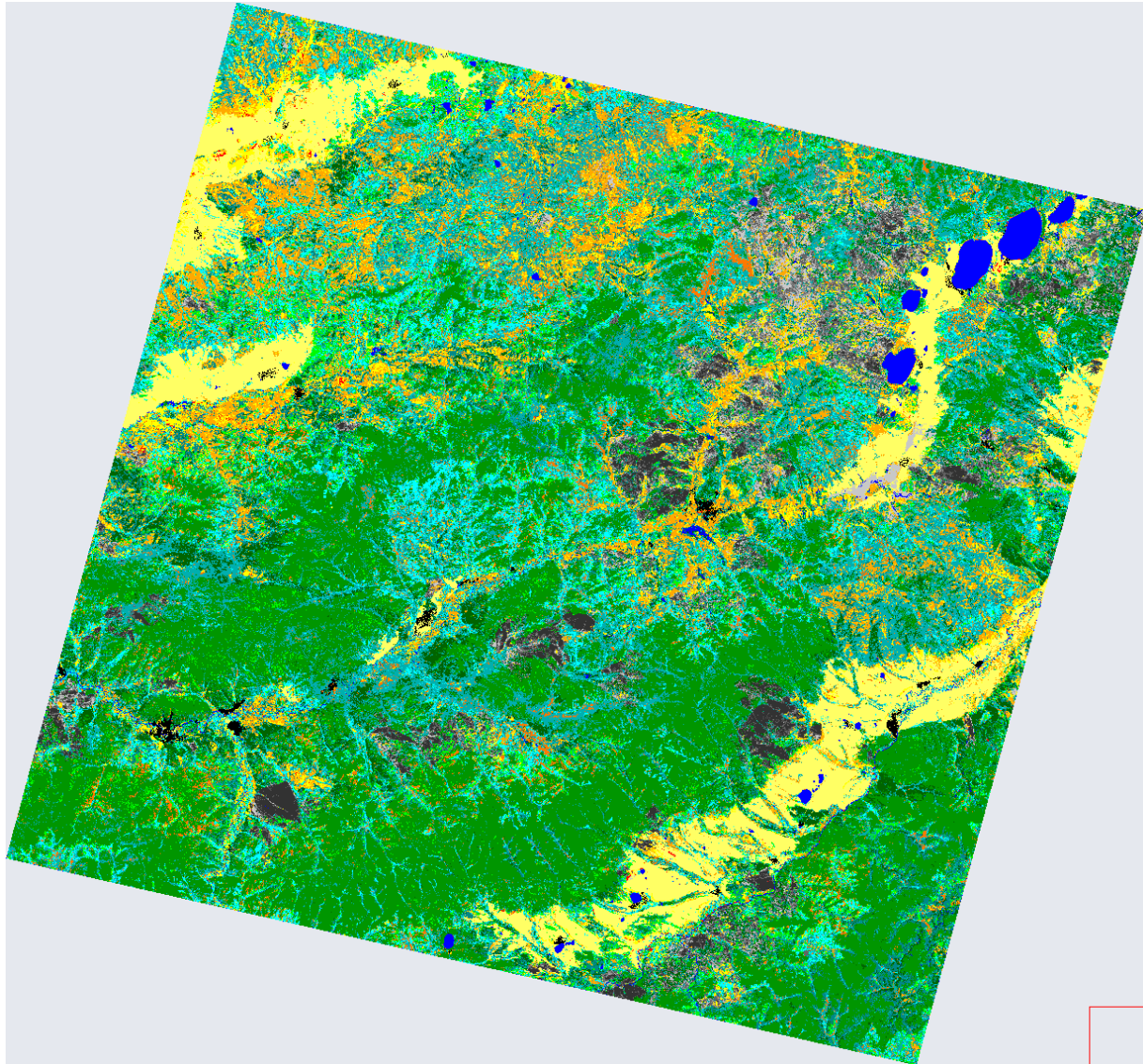
		Observed Class					Sum	Commission
		Trees	Shrubs	Herbaceous	Barren	Water		
Predicted Class	Trees	210	3	3	0	2	218	3.67
	Shrubs	18	26	1	0	0	45	42.22
	Herbaceous	2	7	37	8	0	54	31.48
	Barren	0	0	3	22	0	25	12
	Water	0	0	0	0	32	32	0
	Sum	230	36	44	30	34	374	
Omission		8.7	27.78	15.91	26.67	5.88		
<b>Overall Accuracy = 87.4332%</b>								
<b>Kappa Coefficient = 0.7905</b>								

### 5.4.2 Full classification accuracy assessment

For the accuracy assessment of the full classification all tree mortality classes were collapsed into one “Tree.mortality” thus reducing the total number of classes from 17 to 15. A two-step process of random point selection was implemented for separate classification of 1) tree, shrub, and herbaceous classes; and 2) tree and shrub with mortality, bare, and herbaceous.cultivated classes. Validation points for the “Water” class were adopted from the aggregated accuracy assessment classes. Selection of random points for the first group (including tree, shrub and herbaceous classes) was limited to the extent of the available QuickBird imagery in Google Earth to ensure the ability to differentiate between classes. Random points for the other group (including tree and shrub with mortality, bare, and herbaceous.cultivated classes) were selected across the entire Landsat scene. Random points which were not confidently identified by the analyst were removed from further validation and replaced with a new set of points.

		Observed class														Sum	Commission %
		TNDC	TNDO	TMC	TMO	TBDC	TBDO	TM	SBC	SBO	SMH	HC	BS	BB	W		
Predicted class	unclassified	0	0	0	0	0	0	1	0	0	0	0	0	0	0	1	
	TNDC	<b>48</b>	4	0	1	0	0	0	1	1	0	0	0	0	2	57	15.79
	TNDO	1	<b>24</b>	0	0	0	0	0	0	2	1	0	0	0	0	28	14.29
	TMC	0	0	<b>86</b>	5	5	0	0	1	0	0	0	0	0	0	97	11.34
	TMO	1	1	1	<b>67</b>	1	2	0	3	0	0	0	0	0	0	76	11.84
	TBDC	0	0	1	3	<b>26</b>	1	0	0	0	0	0	0	0	0	31	16.13
	TBDO	0	0	0	0	0	<b>38</b>	0	0	1	0	0	0	0	0	39	2.56
	TM	0	0	0	0	0	0	<b>49</b>	0	0	4	0	0	0	0	53	7.55
	SBC	0	0	0	0	4	1	0	<b>22</b>	3	0	1	0	2	0	33	33.33
	SBO	0	1	0	0	0	0	0	3	<b>31</b>	1	0	0	2	0	38	18.42
	SM	0	0	0	0	0	0	2	0	0	<b>18</b>	0	0	0	0	20	10
	H	0	0	0	0	0	0	0	0	1	6	<b>23</b>	1	2	1	34	32.35
	HC	0	0	0	0	0	0	0	0	0	0	9	<b>34</b>	3	7	53	35.85
	BS	0	0	0	0	0	0	0	0	0	0	0	11	<b>21</b>	0	32	34.38
	BB	0	0	0	0	0	0	0	0	0	0	0	0	1	<b>22</b>	23	4.35
	W	0	0	0	0	0	0	0	0	0	0	0	0	0	<b>32</b>	32	0
	Sum	50	30	88	76	36	42	52	30	39	30	33	46	31	30	34	647
Omission %	4	20	2.27	11.84	27.78	9.52	5.77	26.67	20.51	40	30.3	26.09	32.26	26.67	5.88		
<b>Overall Accuracy = 83.62%</b>																	
<b>Kappa Coefficient = 0.8222</b>																	

## 5.5 Analysis of mapping results



### Land Cover Classes

unclassified	Tree.mortality.low
Tree.needleleaf.deciduous.closed	Tree.mortality.moderate
Tree.needleleaf.deciduous.open	Tree.mortality.high
Tree.mixed.closed	Shrub.deciduous.closed
Tree.mixed.open	Shrub.deciduous.open
Tree.broadleaf.deciduous.closed	Shrub.mortality
Tree.broadleaf.deciduous.open	Herbaceous
	Herbaceous.cultivated
	Bare.sparse
	Bare.built
	Water

The results of the Landsat/ETM+ classification were analyzed as percent of cover within the full extent of the Landsat scene (path 129 row 24). According to the classified image, tree dominated mixed land cover dominates the Chita area (>25%). Overall tree dominated land cover accounts for nearly 75% of the total area; however, more than 4.5% of the total area of the scene is within recent (1998-2000) burns thus representing tree stands with partial or full mortality.

### Distribution of land cover classes

<i>Class</i>	<i>Pixel</i>	<i>Area (ha)</i>	<i>% of site</i>
Tree.needleleaf.deciduous.closed	2027205	164,662	5.307
Tree.needleleaf.deciduous.open	2581583	209,692	6.759
Tree.mixed.closed	9861032	800,972	25.816
Tree.mixed.open	6598700	535,986	17.275
Tree.broadleaf.deciduous.closed	2089891	169,753	5.471
Tree.broadleaf.deciduous.open	3504638	284,668	9.175
Tree.mortality.low	437084	35,503	1.144
Tree.mortality.moderate	742492	60,310	1.944
Tree.mortality.high	632293	51,359	1.655
Shrub.broadleaf.closed	1235878	100,385	3.236
Shrub.broadleaf.open	2716193	220,625	7.111
Shrub.mortality	579770	47,092	1.518
Herbaceous	1769932	143,764	4.634
Herbaceous.cultivated	2885003	234,337	7.553
Bare.sparse	37003	3,006	0.097
Bare.built	113110	9,187	0.296
Water	385850	31,341	1.010

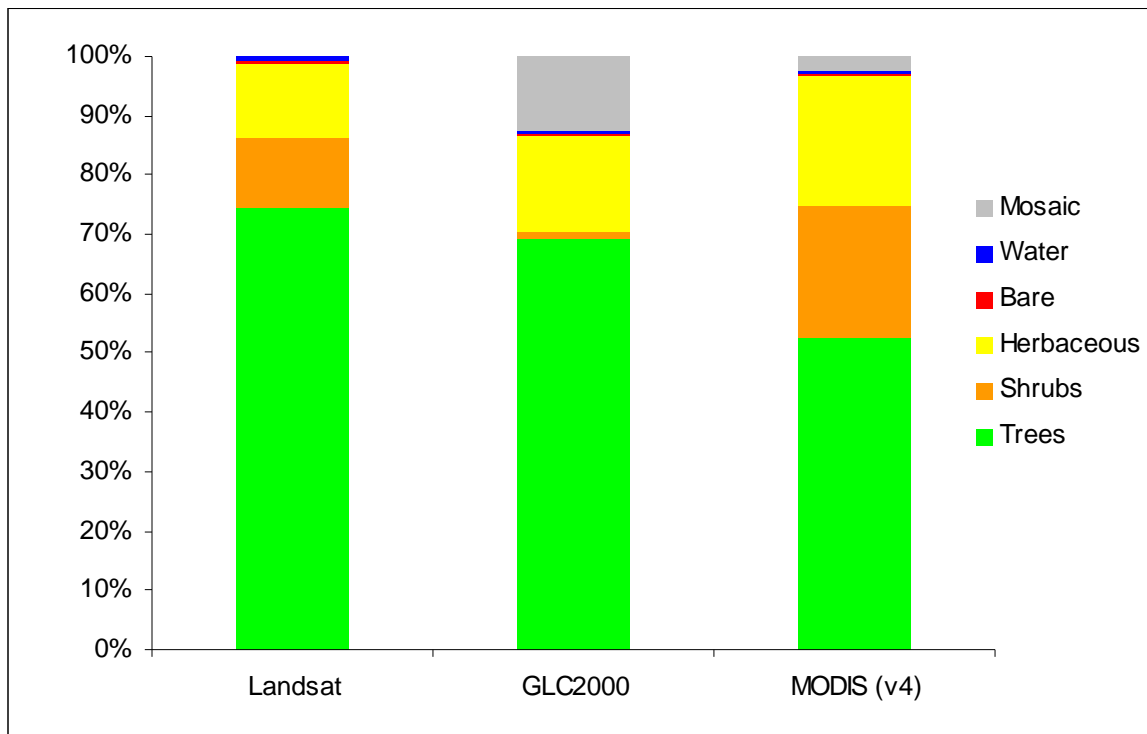
### 5.6 Comparison to coarse resolution land cover maps

The Landsat-based classification results were compared to the several coarse resolution products. Individual classes within each of the products were aggregated to general groups: tree dominated, shrub dominated, herbaceous dominated, bare, water and mosaic/other. IGBP-based classification was used for coarse resolution products. During the aggregation procedure cropland class was mapped as “herbaceous dominated”.

Distribution of aggregated land cover types in the Landsat, GLC2000, and MODIS (MOD12Q1) land cover products (percent):

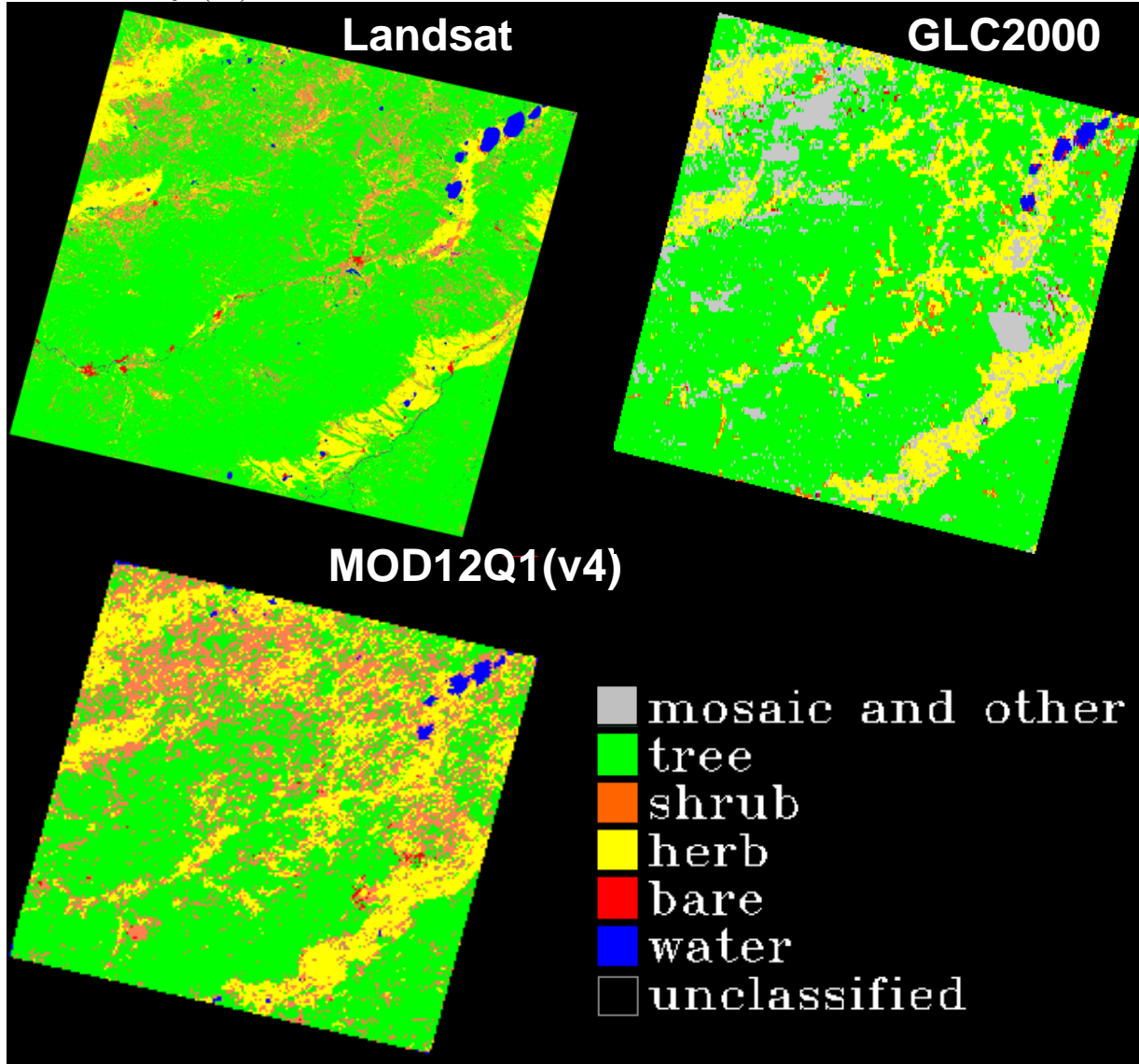
<i>Class</i>	<i>Landsat</i>	<i>GLC2000</i>	<i>MODIS (v4)</i>
Tree dominated	74.546	69.033	52.688
Shrub dominated	11.864	1.252	22.106
Herbaceous dominated	12.186	16.360	21.999
Bare	0.393	0.317	0.210
Water	1.010	0.567	0.742
Mosaic and other	N/A	12.472	2.255

Percent land cover within the extent of the Landsat scene (path 129 row 24) mapped by the ETM+, GLC2000, and MOD12Q1 (v4).





Spatial variations in distribution of aggregated land cover types mapped by ETM+, GLC2000, and MOD12Q1 (v4).



## 6 Land Cover Change Map

### 6.1 Pre-processing

Three Landsat TM and ETM+ scenes for the study site were selected to use in change detection mapping: a) May 29, 1992, b) June 11, 2000; c) August 7, 2006 (see section 2.1). Each of the scenes was visually examined to determine its acquisition during the “leaf on” season. The scenes were converted to surface reflectance and orthorectified using the LEDAPS processing stream (see section 5.1). Finally, the scenes were additionally geometrically co-registered to the scene from June 6, 2000 with  $RMS < 0.5$ .

### **6.1.1 Mature forest mapping**

Water, shadow, cloud, and “mature forest” (defined by the analyst) were identified in the imagery. First, shadow, clouds, and water masks were created using band thresholding and subsequent analyst-driven selection. Second, multivariable stacks including surface reflectance for bands 1-5 and 7, thermal band (6), NDVI, NBR, and Tasseled Cap (TC) transforms (using surface reflectance coefficients (Crist, 1985)) for brightness, greenness, and wetness parameters were compiled for each scene. Third, maximum likelihood classification for bare, sparsely vegetated, shrub, and tree classes with a 0.7 probability threshold was run on the 1992 and 2006 scenes masking out classes identified in step 1. Mature forests for 2000 image were identified based on the detailed classification including all tree dominated classes with the exception of “tree dominated with mortality” class.

### **6.1.2 Accuracy assessment for mature forest mapping**

The results of the maximum likelihood classification for 1992 and 2006 scenes were compared to in situ forest inventory data to provide the accuracy assessment of the “mature forest” layer. Pre-processing of the forest inventory data is described in the classification section. For the purpose of accuracy assessment the in situ data were “aged” to match the forest structure at the time of image acquisition. Tree dominated stands which were  $\geq 30$  years of age at the time of image acquisition were included in the “tree validation” data set. The “shrubs” dominated dataset included only areas dominated by dwarf birch and thus representing a non-successional shrub type. The results of the classification were compared to these forest inventory subsets to assess the overall mapping accuracy and analyze the source of disagreement between the two data sources.

#### **6.1.2.1 Scene from May 29, 1992**

The mapped “shrubs” class corresponded well to the in situ observations with ~ 89% overall accuracy. Approximately 9% of areas designated as “shrubs” forest inventory were mapped as “sparse/damaged vegetation” class, and ~ 2% were mapped as “tree dominated” class.

The “tree” class shows less consistency in the comparison with forest inventory data. Only 66% of areas identified as “tree dominated” in the inventory data corresponded to the mapped “tree” class with 21% mapped as “shrubs” and 13% mapped as “sparse/damaged vegetation”. Further analysis demonstrated that the primary source of disagreement between the forest inventory and classified data sets were driven by low percent crown cover of the forest stands noted in the forest inventory data. Over 76% of pixels classified as “shrubs” and ~77% of pixels classified as “sparse of damaged vegetation” which fall within “tree dominated” forest inventory stands have crown density of  $\leq 60\%$ .

Overall the results of the accuracy assessment show that the produced map of “mature forest stands” required for further disturbance analysis is representative of closed canopy stands characteristic for the study area and subsequently sufficient for further analysis.

### 6.1.2.2 Scene from August 7, 2006

Development of validation data set for the accuracy assessment of the maximum likelihood classification based on the 2006 image presented additional difficulties. The forest inventory data included in this work were compiled for January of 2003 (Hiloksky leskhoz) and January of 2004 (Badinsky leskhoz). The auxiliary data from the MODIS fire detections indicates a very large fire year in 2003 and smaller fire events in subsequent years. Therefore the data compiled for the beginning of 2003 and 2004 are not representative of potential changes in the land cover and forest stands which occurred by the time of the image acquisition in August of 2006. Based on the differences between the collection time for the forest inventory data and the image acquisition, the classification of “tree dominated” or “shrub dominated” inventory polygons as “sparse/damaged vegetation” should not be considered as a misclassification error. The main focus of the accuracy assessment is subsequently placed on the ability of the classification of differentiate between “shrub” and “tree” dominated land covers.

The mapped “shrub” class corresponded to 55% of the “shrub dominated” area in the forest inventory data with 31% mapped as “sparse/damaged vegetation” and 7% mapped as the “tree” class.

The “forest dominated” field reference polygons were mapped as the “tree” class for 30% of the area, as the “shrub” class for 15% of the area and as the “sparse/damaged vegetation” for 50% of the area. The remaining 5% of the field reference data were fell within the “cloud and shadow” mask. 50% of the areas mapped as “shrub” are found within forest stands with  $\leq 60\%$  crown cover. It is unclear if the crown density of the remaining 50% of tree stands mapped as “shrub” was consistent with the in situ observations of the data inventory years.

Overall the results of the accuracy assessment show little confusion of field designated “shrub dominated” landscapes with the “tree” class. However, there is a considerable amount of discrepancy between designated “tree dominated” landscapes and the extent of the “tree” class. These areas are mapped as “shrub” in 15% of the cases. Because of the differences in the time frame for image acquisition and field data inventory compilation it is unclear whether the observed differences represent a misclassification error or reflect the actual biophysical change of the land covers in the study area. The accuracy assessment suggests that the classification results of the “mature tree” mapping present a conservative estimate of mature tree stands in the area. However, the spectral signature within the resultant mask is representative of the reflectance properties of the “mature tree” class required for further disturbance mapping.

## 6.2 Change detection

Change detection was based on the Disturbance Index (DI) methodology developed by Healy et al. (2005). The “mature forest” masks (section 6.1.1) were used to normalize the TC brightness, greenness, and wetness components to that of the mature forests following

$$\begin{aligned}B_r &= (B - B_\mu) / B_\sigma \\G_r &= (G - G_\mu) / G_\sigma \\W_r &= (W - W_\mu) / W_\sigma\end{aligned}$$

where  $B_r$ ,  $G_r$ ,  $W_r$  is rescaled Brightness, Greenness and Wetness,  $B_\mu$ ,  $G_\mu$ ,  $W_\mu$  is mean Brightness, Greenness, and Wetness of “mature forest”, and  $B_\sigma$ ,  $G_\sigma$ ,  $W_\sigma$  is standard deviation of Brightness, Greenness, and Wetness in “mature forest”.

The DI is then calculated following

$$DI = B_r - (G_r + W_r)$$

The common extent of the three scenes was defined and tree cover change was assessed using the maximum likelihood classification of the multi-temporal DI stack (1992-2000-2006). The training data was selected by the analyst based on visually identifiable disturbance and regrowth patterns within the three scenes. Fore change was mapped only within areas identified as “tree dominated” during any of the mapping years, i.e. 1992, 2000 or 2006. Areas with other dominant land cover types were masked out.

### **6.3 Post-classification processing**

A 5-consecutive pixels minimum filter is run to eliminate potential noise of the resultant change. The eliminated pixels were filled using the iterative majority analysis within a 5X5 kernel.

### **6.4 Accuracy assessment**

Two accuracy assessment approaches were applied to change detection. The first approach follows the random pixel selection and analyst interpretation described in section 5.4. However, the resultant change detection classes are not necessarily mutually exclusive. For example, a disturbance between years 1992 and 2000 can be also classified as regrowth between 2000 and 2006. This condition leads to increased uncertainty in the analyst’s ability to assign the final class correctly. Consequently, a second accuracy assessment scheme based on analyst driven selection of validation sample pixels is offered in section 6.4.2.

#### **6.4.1 Random selection accuracy assessment**

The distribution of accuracy assessment points was split by ~150 pixels for “unchanged” and ~150 pixels for “changed” classes. Within each of the classes, the number of validation pixels was assigned proportionally to the class size but no less than 30 pixels. Identification of regrowth pixels between years 2000 and 2006 was particularly challenging due the low overall numbers of pixels in this class (see section 6.5). The analyzed classes include: 1) unchanged non-forest (UNF), 2) unchanged forest (UF), 3) disturbance between 1992 and 2000 (D2000), 4) regrowth between 1992 and 2000 (R2000), 5) disturbance between 2000 and 2006 (D2006) and regrowth between 2000 and 2006 (R2006).

Predicted class	Observed class						Sum	Commission %
	UNF	UF	D2000	R2000	D2006	R2006		
Unclassified	0	0	0	2	0	0	2	
UNF	<b>81</b>	0	8	5	8	13	115	29.57
UF	0	<b>56</b>	1	1	0	0	58	3.45
D2000	1	1	<b>30</b>	0	4	0	36	16.67
R2000	5	1	3	<b>30</b>	7	3	49	38.78
D2006	1	2	2	2	<b>58</b>	1	66	12.12
R2006	1	0	4	13	0	<b>13</b>	31	58.06
Sum	89	60	48	53	77	30	357	
Omission %	8.99	6.67	37.5	43.4	24.68	56.67		

**Overall Accuracy = 75.07%**  
**Kappa Coefficient = 0.6927**

#### 6.4.2 Analyst driven selection accuracy assessment

A second accuracy assessment was conducted against analyst selected samples collected from Landsat ETM+ and TM surface reflectance imagery for years 1992, 2000, 2002, 2003, 2004, 2005, and 2006. The analyst selected 5 validation samples (independent of the training samples) visible in the time series of surface reflectance imagery (independent of the change detection map). The “unchanged non-forest” class (UNF) was primarily selected from the visually identifiable in all images agricultural fields. The “unchanged forest” class (UF) was selected if it was visually identified as “forest” by the analyst in 1992, 2000 and 2006 images. The “disturbance 1992-2000” class (D2000) was selected from visually identified burns and logged sites between 1992 and 2000 images. The “disturbance 2000-2006” was identified from burns visible in 2003, 2004, and 2005 images and logged areas identifiable between 2000 and 2006 images. Although forest regrowth was mapped for both 1992-2000 and 2000-2006 periods, it was very difficult to visually identify the time frame when the class switched to “tree dominated”. Consequently, both classes were combined into “regrowth between 1992 and 2006” class (R2006) for accuracy assessment. The validation samples for this class were visually identified in the 1992-2000-2006 stack to insure that only areas of continuing regrowth throughout the entire time were selected to avoid potential confusion with disturbance classes.

Predicted class	Observed class					Sum	Commission %
	UNF	UF	R2006	D2006	D2000		
UNF	4534	0	29	146	59	4768	4.91
UF	0	5881	0	0	0	5881	0
R2006	0	59	1147	0	0	1206	4.89
D2006	0	0	25	2106	0	2131	1.17
D2000	0	0	0	3	2686	2689	0.11
<b>Sum</b>	4534	5940	1201	2255	2745	16675	
<b>Omission %</b>	0	0.99	4.5	6.61	2.15		

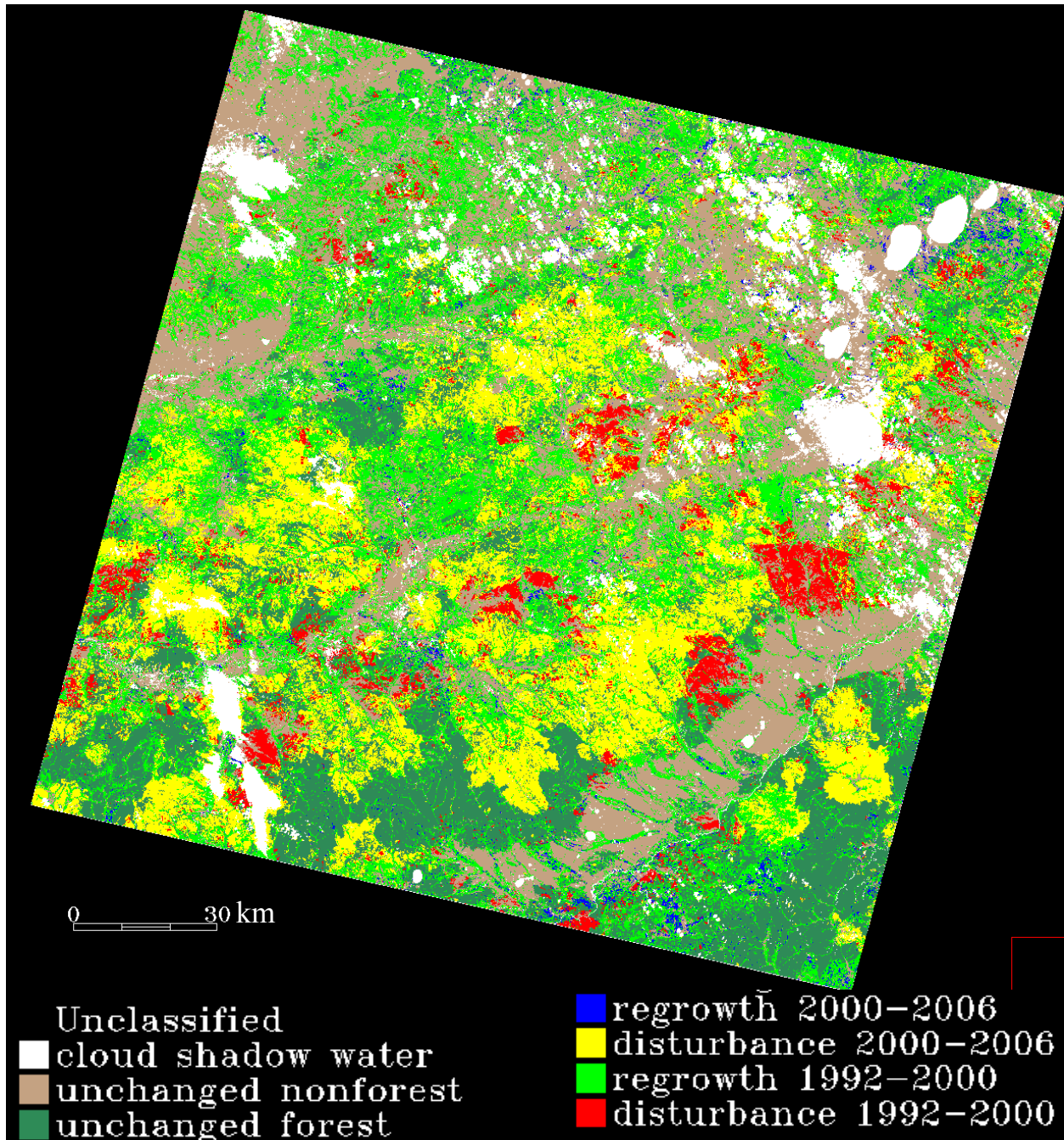
**Overall Accuracy = 98.0750%**

**Kappa Coefficient = 0.9742**

## 6.5 Results of the land cover change map

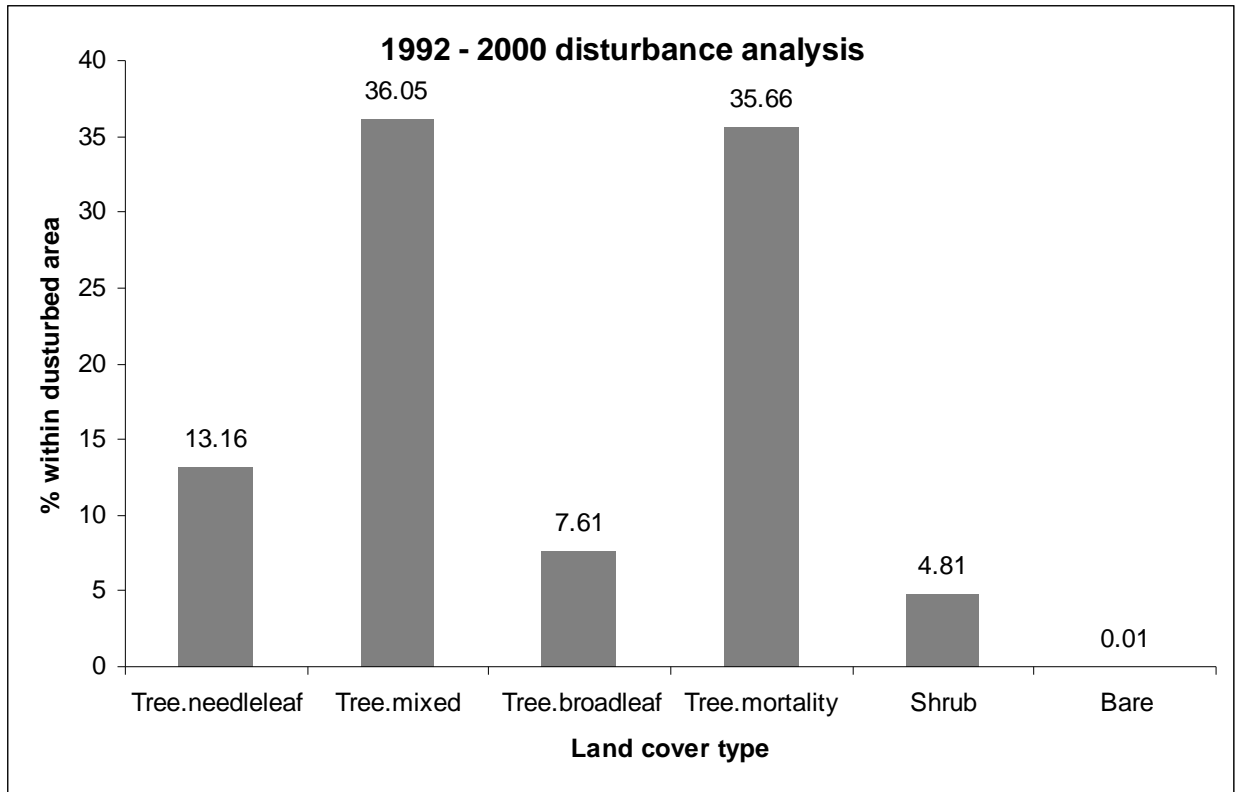
Visual analysis of change detection results indicates that the extensive forest regrowth mapped between 1992 and 2000 may in part be driven by the phenological differences in vegetation development. Although the images for the two dates were acquired within 12 calendar days of each other (5/29/1992 and 6/11/2000) the interannual variability in the onset of the green-up or possibly variation in temperatures and precipitation resulted in visible differences in greenness of vegetation dominated landscapes between the two dates. Therefore, the analysis may overestimate forest regrowth between 1992 and 2000.

<i>Class</i>	<i>Pixels</i>	<i>Area (ha)</i>	<i>% study area</i>
masked pixels	3251912	264,136.55	8.75
unchanged nonforest	9601906	779,914.81	25.84
unchanged forest	5883135	477,857.64	15.83
regrowth 2000-2006	600256	48,755.79	1.62
disturbance 2000-2006	6405909	520,319.96	17.24
regrowth 1992-2000	9652632	784,035.03	25.98
disturbance 1992-2000	1761860	143,107.08	4.74



## 6.6 Analysis of the land cover change map

The analysis of the 1992-2000 disturbed areas in comparison with land cover distribution mapped from 2000 image shows that nearly 93% of disturbed areas returned to or remained within tree dominated land cover types, including ~13% in tree.needleleaf classes, ~36% in tree.mixed classes, nearly 8% in tree.broadleaf classes and nearly 36% in tree with mortality classes. Nearly 66% of these tree dominated with mortality stands were classified as forests with > 60% mortality. Nearly 5% of disturbed tree dominated areas became shrub dominated communities and ~3% were classified as herbaceous.



The analysis of disturbances between 2000 and 2006 showed that nearly 97% of affected areas were within tree dominated stands with ~16% within tree.needleleaf class, ~73% within tree.mixed class and ~7% within tree.broadleaf class. According to the results, ~46% of all needleleaf, ~51 % of all mixed, and ~20% of broadleaf tree dominated stands in the study area were affected by disrurbances between 2000 and 2006, with the majority of disturbances occurring during the extreme 2003 fire season. Over 11% of stands with mortality mapped for the year 2000 were subsequently affected by burning in 2003 with the majority (over 73%) of stands affected found within tree.mortality.low class

The results indicate that between 1992 and 2006 forest dominated landscapes experienced considerable change both in terms of disturbance and forest gain. The data shows that only 42% of all needleleaf, 47% of mixed, and 16% of broadleaf tree dominated communities and 7% of shrub dominated communities did not change between 1992 and 2006.



## 7 Publications Using the Site Data

Loboda, T.V., Csiszar, I.A., et al. (in preparation). Monitoring fire-induced land cover change and post-fire vegetation recovery in Southern Siberia using multi-sensor mapping capabilities. Planned for submission to the *Remote Sensing of Environment*.

Loboda, T.V., Potapov, P., Krankina, O., et al. (in preparation). Evaluation of efficiency of mapping forest disturbance at the continental scale in Northern Eurasia from coarse resolution sensors. Planned for submission to the *Remote Sensing of Environment*.

## 8 List of Contributors to Site Data and Report

Tatiana V. Loboda

University of Maryland  
Geography Department  
2181 LeFrak Hall  
College Park, MD 20742

Ivan A. Csiszar

NOAA/NESDIS  
Center for Satellite Applications and Research  
5200 Auth Rd., Rm 711  
Camp Springs, MD 20746

## 9 Acknowledgements

This research was supported by the NASA Land Cover Land Use Change Program Grant # NS175AA. The researcher would also like to thank Dr. Jeff Masek for his help in pre-processing data through the LEDAPS system.

## 10 References

Crist, E.P. (1985). A TM Tasseled Cap Equivalent Transformation for Reflectance Factor Data. *Remote Sensing of Environment* **17**, 301-306.

Healy, S.P., Cohen, W.B., Zhiqiang, Y., Krankina, O.N. (2005). Comparison of Tasseled Cap-based Landsat data structures for use in forest disturbance detection. *Remote Sensing of Environment* **97**, 301-310.

Key, C. H., & Benson, N. C. (1999). Measuring and remote sensing of burn severity. In L. F. Neuenschwander, K. C. Ryan, & G. E. Goldberg, (Eds.), Proceedings of the Joint Fire Science Conference, Boise, Idaho 15–17 June, 1999. University of Idaho and the International Association of Wildland Fire, vol. II (p. 284).

Loboda, T., O’Neal, K.J., Csiszar, I. (2007). Regionally adaptable dNBR-based algorithm for burned area mapping from MODIS data. *Remote Sensing of Environment* **109**, 429-442.

Stolbovoi V, McCallum I (2003) Land Resources of Russia. CD-Rom. International Institute for Applied Systems Analysis and the Russian Academy of Science. Laxenburg, Austria.